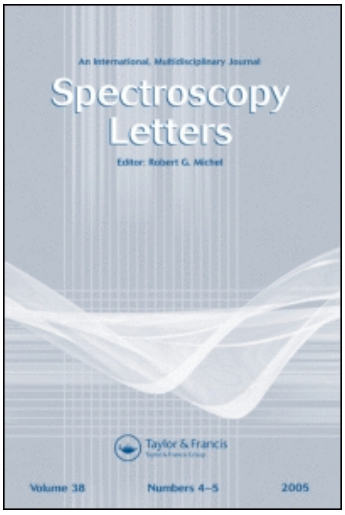

Spectroscopy Letters
Publication details, including instructions for authors and subscription information:
http://www.informaworld.com/smpp/title~content=t713597299

Investigation of HgBr($B^2\Sigma$) excitation due to collisions of Kr ions with $HgBr_2$ molecules

Mohammad F. Mahmood[a]
[a] DEPARTMENT OF ELECTRICAL ENGINEERING HOWARD UNIVERSITY, WASHINGTON, DC, USA

To cite this Article Mahmood, Mohammad F.(1990) 'Investigation of HgBr($B^2\Sigma$) excitation due to collisions of Kr ions with $HgBr_2$ molecules', Spectroscopy Letters, 23: 9, 1183 — 1193
To link to this Article: DOI: 10.1080/00387019008054492
URL: http://dx.doi.org/10.1080/00387019008054492

SPECTROSCOPY LETTERS, 23(9), 1183-1193 (1990)

Investigation of HgBr($B^2\Sigma^+$) excitation due to collisions of Kr^+ ions with $HgBr_2$ molecules

MOHAMMAD F. MAHMOOD
DEPARTMENT OF ELECTRICAL ENGINEERING
HOWARD UNIVERSITY, WASHINGTON, DC 20059, USA

Abstract. - Electronic excitation of Hg and the HgBr radical has been observed in the present studies during collisions of $HgBr_2$ with Kr^+ ions at different laboratory kinetic energies. Emission cross-sections for excitation of the most intense band of the HgBr($B^2\Sigma^+$, $v' = 0 \rightarrow X^2\Sigma^+$, $v'' = 22$) transition at 502 nm have been measured in the kinetic energy range of 100-1000 eV.

1. Introduction

There has been a considerable interest in developing highly efficient lasers for use in ocean optics, especially for transmitting communication signals to submarines and for the measurement of ocean depth near the coastal lines [1]. HgBr lasers meet most of the requirements needed for ocean optics. These lasers have been observed to lase in HgBr radical involving low lying vibrational levels of the electronically excited $B^2\Sigma^+$ state and high vibrational levels of

the ground X $^2\Sigma^+$ state during electrical or optical pumping of $HgBr_2$ vapor [2-9]. Since the laser transitions terminate to the high vibrational levels of the ground state, collisional quenching of these levels by gases such as N_2, Ar, Kr, etc. has been proposed to improve the performance of HgBr lasers [10, 11]. In a discharge medium containing these gases along with $HgBr_2$ vapor, a variety of processes such as excitation, ionization, dissociation, etc. take place leading to the formation of excited as well as ionized species. In a discharge medium containing Kr, a large number of Kr^+ ions are expected to be produced due to collisions with electrons. These Kr^+ ions when collide with $HgBr_2$ molecules present in the discharge medium, they contribute to the formation of the $HgBr(B^2\Sigma^+)$ state and atomic mercury lines during collision induced dissociative excitation processes. The $HgBr(B^2\Sigma^+-X^2\Sigma^+)$ emission intensity was observed [12] to be weak during dissociative excitation of $HgBr_2$ by $Kr(^3P_2)$. In this communication, observations are reported on the formation of $HgBr(B^2\Sigma^+-X^2\Sigma^+)$ band system and atomic mercury lines during collisions of $HgBr_2$ with Kr^+ ions at different laboratory kinetic energies. Emission cross sections have also been measured of the most intense band of the $HgBr(B^2\Sigma^+-X^2\Sigma^+)$ transition corresponding to 502 nm at different laboratory kinetic energies of the projectile ions. This information may be useful in theoretical modeling and proper understanding of the kinetics of discharge pumped mercury bromide lasers.

2. Experiment

The experiment was performed by directing a mass selected ion beam of Kr^+ in a collision cell containing $HgBr_2$ vapor. The ions were produced by electron impact on flowing krypton gas through a dc discharge operating at low voltage. The ions were extracted from a small hole in the anode, accelerated to an energy of about 1 keV and focused into a high resolution Wien velocity filter [13] by means of a set of Einzel lenses. The desired mass-selected Kr^+ ions were then de-accelerated by using another set of electrostatic lenses into the collision cell (Fig. 1). The collision cell has a slot (2cm x 2mm) parallel to the ion beam and equipped with a sliding suprasil window for monitoring the emitted photons due to the ion-molecule reactions inside the collision cell. This cell has two apertures for entrance and exit of the ion beam. The mercury bromide vapor was generated by heating $HgBr_2$ salt in a container underneath collision cell. The container was made of copper and wrapped with a band heater. The temperature of the mercury bromide vapor was measured by a calibrated thermocouple (k-type, Keithley Insturments) and was displayed on a digital thermometer. This temperature was then used to calculate the vapor density of $HgBr_2$. Ions were collected on a Faraday cup connected to a sensitive electrometer to measure ion currents. The Kr^+ ion current was observed to be in the range of 1nA to 1 μA in the kinetic energy range of 100 - 1000 eV. The ion source, Wien velocity filter, collision cell, $HgBr_2$ vapor generator, and ion collector (Faraday cup) were all housed in a stainless

steel chamber. This chamber was evacuated by two mechanical pumps and a cryogenic pump (CTI model Cryo-Torr-8) to a base pressure of about 10^{-7} Torr. The chamber pressure was monitored by a calibrated Bayer-Lampert ionization gauge. The resulting atomic and molecular emission photons were monitored in a direction perpendicular to the ion beam. The light emitted from the collision cell due to ion-molecule reactions involving $Kr^{\cdot}$ and $HgBr_2$ molecules was dispersed by a 0.2m scanning monochromator (McPherson model 275 attached to a scanner model 789) and detected by a cooled (-25°C) photomultiplier tube (PMT) (EMI GenCom model 9863 QB/5). The output of the PMT was amplified and displayed on a photon counter (EMI Gen Com model AD-100 amplifier and C-10 counter). The output signal from the photon counter was sent to a multichannel analyzer (MCA) (Norland Corporation model 5680) for storage and plotting data.

3. Results and discussion

Emission spectra of the ($B^2\Sigma^{\cdot} - X^2\Sigma^{\cdot}$) transition of HgBr radical as well as mercury atomic lines from energy levels as high as Hg(6 ^{3}D) to various lower energy levels, according to the electric dipole selection rule $\Delta J = 0, \pm 1$, were observed in the wavelength range 580 - 300 nm during collisions involving $Kr^{\cdot}$ ions at various kinetic energies (lab.) and $HgBr_2$ molecules. In the case of $Ar^{\cdot}$ and $HgBr_2$ collisions, it was possible to observe HgBr($B^2\Sigma^{\cdot} - X^2\Sigma^{\cdot}$) emission bands and atomic mercury lines at kenetic energies as low as 10 eV, whereas with $Kr^{\cdot}$ and $HgBr_2$ collisions, these emissions were not observed below 100 eV under similar

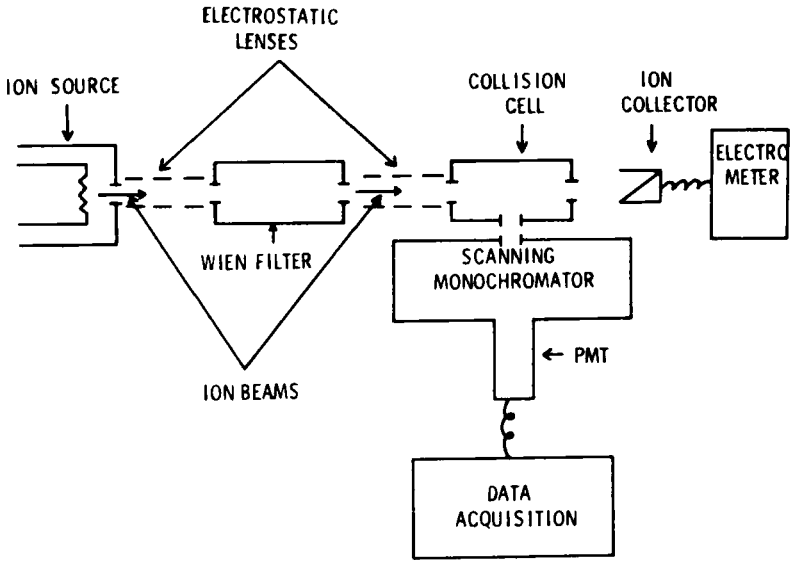

Figure 1 Experimental setup used in the present study.

experimental conditions Figure 2 shows the emission spectra of the HgBr ($B^2\Sigma^+$-$X^2\Sigma^+$) band system and atomic mercury lines which were observed during collisions of Ar^+ and Kr^+ ions at a laboratory kinetic energy of 700 eV with $HgBr_2$ molecules at a vapor density of about 0.15 Torr.

The following set of collision-induced dissociative excitation processes may be proposed to explain the observation of HgBr($B^2\Sigma^+$-$X^2\Sigma^+$) band system and highly-excited states of atomic mercury transitions during collisions of Kr^+ ions with $HgBr_2$ molecules.

$$Kr^+ + HgBr_2 \rightarrow HgBr_2(b^{1,3}\Sigma) + Kr^+ + \Delta E \ (-6.30 \text{ eV}) \qquad (1)$$

$$Kr^+ + HgBr_2 \rightarrow HgBr(B^2\Sigma^+) + Br + Kr^+ + \Delta E \ (-6.07 \text{ eV}) \qquad (2)$$

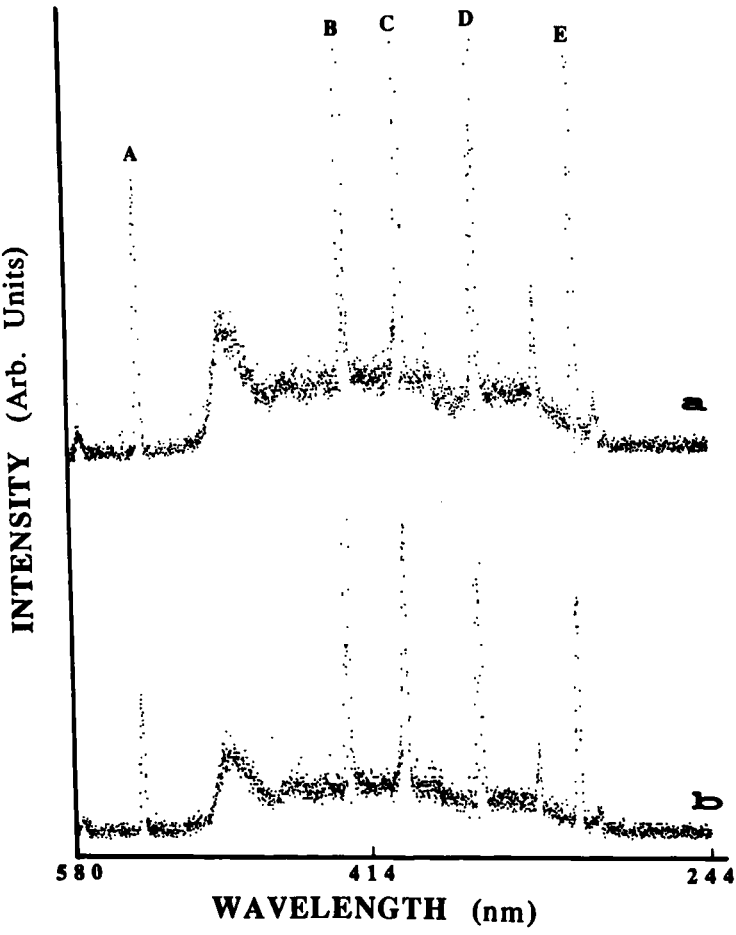

Figure 2 Emission spectra observed during collisions of $HgBr_2$ molecules (≈ 0.15 Torr) and Ar^+/Kr^+ ions at a laboratory kinetic energy of 700 eV.

A = $Hg(7\ ^3S_1\text{-}6^3P_2)$ B = $Hg(7\ ^3S_1\text{-}6^3P_1)$,

C = $Hg(7\ ^3S_1\text{-}6^3P_0)$ D = $Hg(7\ ^3D_3\text{-}6^3P_2)$,

E = $Hg(7^3D_2\text{-}6^3P_1)$

a: $Ar^+ + HgBr_2$ b: $Kr^+ + HgBr_2$

$$Kr^{*}+HgBr_2 \rightarrow Hg^{*}+Br_2+Kr^{*}+ \Delta E\ (-6.78\ eV) \quad (3)$$

$$Kr^{*}+HgBr \rightarrow HgBr(B^2\Sigma^{*})+Kr^{*} + \Delta E\ (-2.92\ eV) \quad (4)$$

$$Kr^{*}+Hg \rightarrow Hg^{*}+Kr^{*}+ \Delta E\ (-4.9\ eV) \quad (5)$$

$$Kr^{*}+Hg^{*} \rightarrow Hg^{**}+ Kr^{*}+ \Delta E\ (-2.86\ eV) \quad (6)$$

where $Hg^{*} = Hg(6\ ^3P_1)$ and $Hg^{**} = Hg(7^3S_1)$ or $Hg(^3D)$. These ΔE values were calculated by using the ground state dissociation energies [14] for the processes $HgBr_2 \rightarrow HgBr+Br$ (3.12 eV), $HgBr_2 \rightarrow Hg + Br_2$ (1.68 eV), and $HgBr \rightarrow Hg + Br$ (0.71 eV). It is because of the low dissociation energies of these ground state species, collision induced dissociative processes will occur before the excitation processes as indicated [see reactions (1) - (6)]. The observation of $HgBr(B^2\Sigma^{*})$ state and atomic mercury lines at 546, 435.8, 404.6, 365 and 312.56 nm from highly excited states of atomic mercury may then be due to the efficient conversion of kinetic energies of Kr^{*} ions into the internal energies of the by product species through the processes (4) - (6), mainly because of their low endothermicities. Such conversions have been observed in the past in other ion-molecules reactions [15].

By using the integrated intensities of the most intense band head of $HgBr(B^2\Sigma^{*}-X^2\Sigma^{*})$ transition at 502 nm corresponding to ($v' = 0 - v'' = 22$), emission cross-sections have been measured at different laboratory kinetic energies of the Kr^{*} ions (see Table I). These cross-sections were calculated by using the following relation:

$$\sigma = I_s/(I_p n L),$$

where σ is the cross-section in cm^2, I_s is the number of

Table 1

Measured emission cross-sections of HgBr($B^2\Sigma^+$, $v' = 0$ - $X^2\Sigma^+$, $v'' = 22$) formation due to Kr^+ and $HgBr_2$ collisions at different laboratory kinetic energies of the projectile ions.

Kinetic energy (eV)	Cross section ($x10^{-16}cm^2$)
1000	0.12
900	0.61
700	1.91
500	1.65
300	0.98
100	0.31

photons/sec, I_p is the number of primary ions/sec, n is the number density of $HgBr_2$ molecules in cm^{-3}, and L is the interaction length (2 cms) of the ion beam with $HgBr_2$ vapor inside the collision cell. It is to be noted here that I_s is the number of photons/sec corrected for the detection efficiency of the optical system including the solid angle of light collection. I_p is the absolute ion current measured at the Faraday cup. The vapor density of $HgBr_2$ molecules at a particular temperature was calculated by using the

thermodynamical constants [16]. The accuracy of these measured cross-sections depends upon the accuracy of measurement of I_s and n. The optical system was calibrated using calibrated lamp traceable to NBS in the wavelength range of 300-800 nm and rechecked by measuring the emission cross-sections of the hydrogen atomic lines observed in charge transfer reactions involving He^+ and H_2 gas at laboratory kinetic energies of 100 and 700 eV. These cross-sections were about 20% higher than those measured in the past [17]. The emission cross-sections of the most intense band of the $HgBr(B^2\Sigma^+, v' = 0 \rightarrow X^2\Sigma^+, v'' = 22)$ transition at 502 nm have been calculated in the laboratory kinetic energy range 100 - 1000 eV of the projectile ions with an estimated accuracy of 20 to 30%.

4. Conclusion

In conclusion, ion-molecule reactions involving collisions of $HgBr_2$ and Kr^+ ions have been studied and have measured the emission cross-sections of $HgBr(B^2\Sigma^+, v' = 0 - X^2\Sigma^+, v'' = 22)$ formation at different kinetic energies. Collision-induced dissociative excitation processes seem to be the dominant mechanism in producing these emissions.

Acknowledgment

The technical assistance of Bill Pinkney and Eugene Jones is gratefully acknowledged.

References

[1] SVANBERG S., Contemp. Phys. 21 (1980) 576.

[2] PARKS J.H., Appl. Phys. Lett. 31 (1977) 297.

[3] SCHIMITSCHEK E.J., CELTO J.E. and TRIAS J.A., Appl. Phys. Lett. **31** (1977) 608.

[4] NIGHAN W.L., HINCHEN J.J. and WIEGAND W.J., J. Chem. Phys. **77** (1982) 3442.

[5] BURNHAM R., Appl. Phys. Lett. **33** (1978) 156.

[6] KVASNIK F. and KING T.A., Appl. Phys. B **28** (1982) 129.

[7] McGEOCH M.W., HSIA J.C. and KLIMEK D.E., J. Appl. Phys. **54** (1983) 3723.

[8] KUSHNER M.J., PINDROH A.L., FISHER C.H., ZNOTINS T.A. and EWING J.J., J. Appl. Phys. **57** (1985) 2406.

[9] SHAY T.M., GOOKIN D., JORDAN M.C., HANSON F.E. and SCHIMITSCHEK E.J., I.E.E.E. J. Quant. Electron. QE-**21** (1985) 1271.

[10] HELVAJIAN H., MANGIR M. and WITTIG C., Chem. Phys. Lett. **71** (1980) 177.

[11] HELVAJIAN H. and WITTIG C., J. Chem. Phys. **76** (1982) 3505.

[12] CHANG R.S.F. and BURNHAM R., Appl. Phys. Lett. **36**(1980) 397.

[13] WAHLIN L., Nucl. Inst. Methods. **27** (1964) 55.

[14] COOL, T.A., McGARVEY J.A. and ERLANDSON A.C., Chem. Phys. Lett. **58** (1978) 108.

[15] KELLEY J.D., BEARMAN G.H., HARRIS H.H. and LEVENTHAL, J.J., J. Chem Phys. **68** (1978) 3345.

[16] KUBASCHEWSKI O. and ALCOCK C.B., Metallurgical Thermochemistry, 5th ed., Pergamon Press, New York (1979) 364.

[17] ISLER R.C. and NATHAN R.D., Phys. Rev. A6 (1972) 1036.

Date Received: 06/18/90
Date Accepted: 07/23/90